

**Half-life and magnetic moment of the first excited state in  $^{132}\text{I}$** M. Tanigaki,<sup>1,\*</sup> S. Izumi,<sup>2</sup> H. Ouchi,<sup>2</sup> A. Sasaki,<sup>2</sup> Y. Miyashita,<sup>2</sup> N. Sato,<sup>2</sup> S. Hoshino,<sup>2</sup> K. Shimada,<sup>3</sup>  
T. Wakui,<sup>3</sup> T. Shinozuka,<sup>3</sup> and Y. Ohkubo<sup>1</sup><sup>1</sup>*Research Reactor Institute, Kyoto University, Kumatori, Osaka 590-0494, Japan*<sup>2</sup>*Graduate School of Science, Tohoku University, Sendai, Miyagi 980-8578, Japan*<sup>3</sup>*Cyclotron and Radioisotope Center, Tohoku University, Sendai, Miyagi 980-8578, Japan*

(Received 1 May 2009; revised manuscript received 26 June 2009; published 3 September 2009)

The half-life and the magnetic moment were measured for the first excited state in  $^{132}\text{I}$ , of which the inconsistent results on the half-life have been reported by several other groups. This time, measurements were performed on  $^{132}\text{I}$  obtained as a decay product of a  $^{132}\text{Te}$  radioactive beam from the ion guide at Tohoku University. The half-life of this level was determined to be  $T_{1/2} = 1.120 \pm 0.015$  ns using a conventional coincidence technique with a pair of  $\text{BaF}_2$  detectors. The time-differential perturbed angular correlation technique was successfully applied to the first excited state in  $^{132}\text{I}$  implanted into nickel foils. The magnetic moment of this state was determined to be  $\mu = +(2.06 \pm 0.18)\mu_N$ . The present results are consistent with values reported by Gorodetzky *et al.* and Singh *et al.*

DOI: [10.1103/PhysRevC.80.034304](https://doi.org/10.1103/PhysRevC.80.034304)

PACS number(s): 21.10.Ky, 21.10.Tg, 27.60.+j, 29.38.-c

**I. INTRODUCTION**

Recent progress in shell-model calculations enables the detailed discussions on the nuclei around doubly closed shells in heavier nuclei. For example, Brown *et al.* recently performed such a microscopic study on nuclei around  $^{132}\text{Sn}$  [1], and measurements of the magnetic moments have been stimulated [2–4] to meet such progress in theory in this region.

In the region around  $^{132}\text{Sn}$ , there have been a long-time confusion on half-life measurements of the first excited state in  $^{132}\text{I}$  since it was originally reported by Gorodetzky *et al.* [5]. Several groups [5–7] reported various results, ranging from 0.96 ns [5] to 7.14 ns [6]. Singh *et al.* reported on the magnetic moment of this state as being  $\mu = +(2.22 \pm 0.30)\mu_N$  [8], determined by the time-integral perturbed angular correlation technique (TIPAC). In this technique, the reliability of the lifetime is crucial, because the Larmor frequency is obtained as the rotation angle of the spin alignment during the lifetime of the investigated state. Considering this confusion on the half-life of this state, their result should be treated as containing a large ambiguity.

From the view of material science, iodine plays an important role in realizing new functions in such substances as glass with high conductivity. Regardless of its importance in material science, few probe nuclei for the perturbed angular correlation technique (PAC) are available in the halogen family. Sato *et al.* recently showed  $^{19}\text{F}$  ( $\leftarrow ^{19}\text{O}$ ) as to be a usable probe for PAC [9,10]. However, its application to material science is still limited because it requires an online measurement where control of the experimental conditions becomes much more difficult than in an off-line measurement. Therefore, developing a proper iodine probe opens the possibility of microscopic studies with the PAC method. It also provides another valuable halogen probe for such studies.  $^{132}\text{I}$  can be such a good probe for the time differential perturbed angular

correlation method (TDPAC) if the half-life reported by Yousif *et al.* [6],  $T_{1/2} = 7.14$  ns, is true.

This time, we report on our measurements of the half-life and the magnetic moment of this first excited state in  $^{132}\text{I}$ .

**II. EXPERIMENT****A. Preparation of sample**

The first excited state in  $^{132}\text{I}$  was populated by the  $\beta^-$  decay of  $^{132}\text{Te}$  ( $T_{1/2} = 3.204$  d). A simplified decay scheme of  $A = 132$  is shown in Fig. 1. Unlike other experiments where chemical separation was performed,  $^{132}\text{Te}$  was obtained as a radioactive beam of  $A = 132$  from the RF-IGISOL at the Cyclotron and Radioisotope Center (CYRIC) in Tohoku University [11,12]. This is the first successful extraction of a radioactive beam in the region around  $^{132}\text{Sn}$  from this RF-IGISOL. A primary beam of 50 MeV protons from the AVF cyclotron at CYRIC bombarded a 20-mg/cm<sup>2</sup> foil of a natural uranium target in a gas cell of RF-IGISOL to produce  $A = 132$  isotopes through proton-induced fission. The typical intensity of the primary beam was about 1  $\mu\text{A}$ . The mass-separated radioactive isotopes were then kinematically implanted into either aluminum or nickel foil for off-line measurements. The acceleration voltage of RF-IGISOL was 30 kV. The radioactive beam from RF-IGISOL mainly consists of  $^{132}\text{Sb}$  ( $T_{1/2} = 2.79$  m and 4.10 m) and  $^{132}\text{Te}$ , and  $^{132}\text{Te}$  is finally populated in the foil because  $^{132}\text{Sb}$  decays to  $^{132}\text{Te}$  through  $\beta^-$  decay. Beam optimization was performed by observing 103.4-, 696.8-, and 973.9-keV  $\gamma$  rays, followed by the  $\beta^-$  decay of  $^{132}\text{Sb}$ . These  $\gamma$  rays were also used as indexes of the beam intensity during the implantation process. Usually, each implantation was performed for about 50 h. The beam intensity was maintained at 500 ~ 1000 atoms/s in terms of  $^{132}\text{Te}$  accumulation in the foil.

The main contaminations in the sample were radioactive isotopes in adjacent masses of  $A = 132$ , i.e.,  $^{131}\text{Sb}$  ( $T_{1/2} = 23$  min),  $^{131}\text{Te}$  ( $T_{1/2} = 25$  min),  $^{131}\text{I}$  ( $T_{1/2} = 8.02$  d) and  $^{133}\text{I}$

\* [tanigaki@rri.kyoto-u.ac.jp](mailto:tanigaki@rri.kyoto-u.ac.jp)

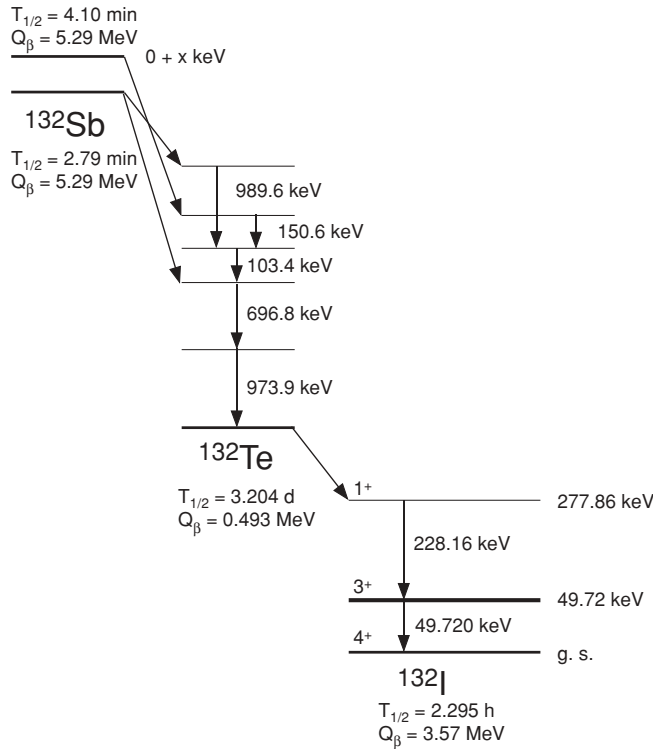


FIG. 1. Simplified decay scheme of the relevant  $A = 132$  mass chain. Transient radioactive equilibrium is realized in the  $^{132}\text{Te} \rightarrow ^{132}\text{I}$  decay by populating  $^{132}\text{Te}$  as the parent nuclei. Only the 277.9-keV state in  $^{132}\text{I}$  is populated by the  $\beta^-$  decay of  $^{132}\text{Te}$ , and the 228.2- to 49.7-keV cascade is dominant in  $^{132}\text{I}$ .

( $T_{1/2} = 20.8$  h). Such contaminations were carefully removed as follows. First, they were attenuated by cooling the sample down for a few hours because of their rather short half-lives compared to  $^{132}\text{Te}$ . After this cooling, the implanted foil was cut into several pieces (typically  $1 \sim 2$  cm<sup>2</sup>), and their energy spectra were measured piece by piece with a Ge detector to select pieces in which  $^{132}\text{Te}$  was dominantly implanted. In this procedure, no explicit shield for background radiations was made. Typical energy spectra of  $\gamma$  rays for selected and discarded pieces are shown in Fig. 2, and a typical energy spectrum for the selected pieces observed by a BaF<sub>2</sub> detector with lead bricks as a shield toward background radiations is shown in Fig. 3.

### B. Half-life of the first excited state in $^{132}\text{I}$

A half-life measurement was performed by a conventional fast-slow coincidence method. A pair of  $1.5 \phi \times 1$ -inch-thick BaF<sub>2</sub> counters were placed face to face with a distance of 2 cm, and then aluminum foils in which  $^{132}\text{I}$  was implanted were placed in between them. As shown in Fig. 3, the  $\gamma$  rays of  $^{132}\text{I}$  were successfully observed and confirmed to be dominant. Other peaks were of  $^{131}\text{I}$  and  $^{133}\text{Xe}$  in the foil, and x rays of lead used for the shield.  $\gamma$  gates were set toward the peaks of 228.2 and 49.7 keV, and triple coincidences of these two  $\gamma$  rays and the TAC signal of these two detectors were collected as true events to generate the time spectrum. Another time spectrum

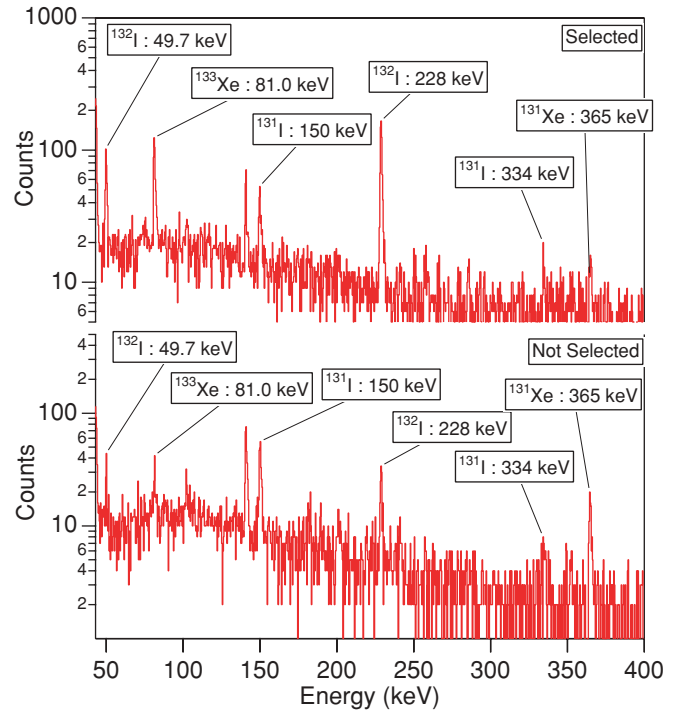


FIG. 2. (Color online) Comparison of typical energy spectra of nickel foils in which  $^{132}\text{I}$  were implanted. “Selected” corresponds to the energy spectrum for a piece used for the measurements and “Not Selected” for a discarded piece, respectively. In this selection procedure, no background shield for the Ge detector was used. The  $\gamma$ -ray peak at 140 keV was identified as a background from other than the foil pieces, possibly from another radioactive source in the laboratory.

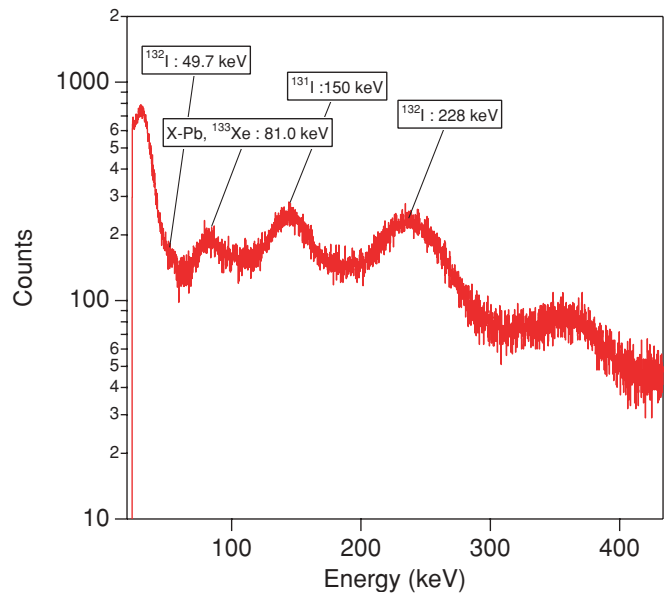


FIG. 3. (Color online) Typical energy spectrum of  $^{132}\text{I}$  implanted into aluminum foil observed by one of the BaF<sub>2</sub> detectors in the present measurement system.  $\gamma$ -ray peaks corresponding to 228 and 49.7 keV were successfully observed. Other peaks were identified as  $\gamma$  rays from  $^{131}\text{I}$ ,  $^{133}\text{Xe}$ , and the x ray from lead bricks that were used for background reduction.

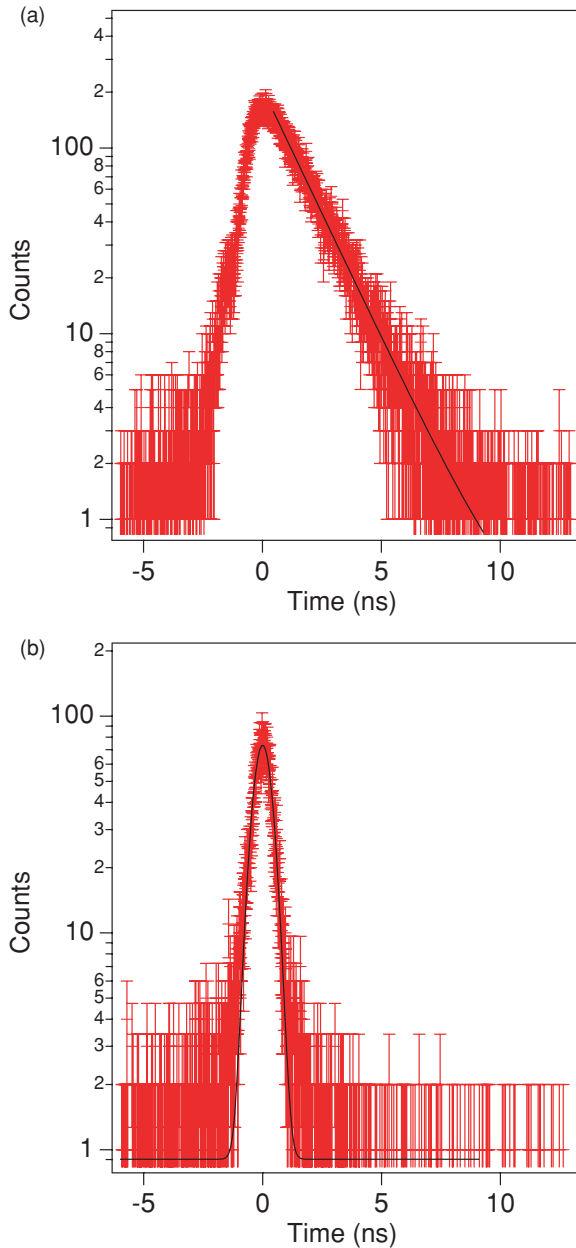


FIG. 4. (Color online) (a) Time spectrum of the 228.2- to 49.7-keV cascade. A single exponential curve with a constant term was applied as a fitting function to the data. The data within the HWHM from the prompt position was excluded from the fit. The solid line is the best fit to the experimental data. (b) Time spectrum taken with the  $\gamma$ -gates shifted slightly above to miss the 228.2- to 49.7-keV cascade. A Gaussian function with a constant term as the fitting function was applied to the data.

was taken by setting the  $\gamma$  gates slightly shifted above so as to miss the respective peaks to estimate the time resolution of the present measurement system. The obtained time spectra are shown in Fig. 4.

Prior to the half-life determination, a sufficient time resolution of 0.9 ns (FWHM) was confirmed in the present measurement system by applying a Gaussian function with a constant term as the fitting function to the time spectrum for

the case of missed peaks. Then, a single exponential curve with a constant term was applied as a fitting function to the data (excluded down to 0.45 ns from the prompt position, corresponding to the HWHM of the time resolution). The half-life of the first excited state in  $^{132}\text{I}$  was determined to be  $T_{1/2} = 1.120 \pm 0.015$  ns.

### C. Magnetic moment of the first excited state in $^{132}\text{I}$

TDPAC measurements were performed on the 228.2- to 49.7-keV  $\gamma$ - $\gamma$  cascade of  $^{132}\text{I}$ . A typical three-counter configuration was used for these measurements. All measurements were performed at room temperature. A pure nickel foil with a thickness of 0.050 mm was used as the implantation medium to apply a strong hyperfine field of iodine at room temperature,  $|B_{\text{hf}}| = 26.5 \pm 0.5$  T [13], thereby carrying out an observable Larmor precession during the confirmed short half-life of this level. The relaxation time of the spin alignment is expected to be considerably longer than those in other measurements of  $A_{22}$  or TIPAC with liquid sources; thus, the present measurement should be free from the relaxation problem in using a solvent source pointed out by Yousif *et al.* [6] After the purification procedure described above, the nickel foils were cut into squares with sizes of about  $1 \times 1$  cm. These cut foils were then placed between a pair of permanent magnets so that the surfaces of  $1 \times 1$  cm were parallel to the external magnetic field. The external magnetic field applied to the sample,  $B_{\text{ext}}$ , was 0.3 T.

Because low-energy  $\gamma$  rays of 49.7 keV participated in the present measurements, a special attention should be paid on the fringing field from the magnet to the  $\text{BaF}_2$  detectors. This time, we have developed a so-called cage type magnet (Fig. 5), which has three return yokes at every  $120^\circ$  to suppress the fringing field at the photocathode of  $\text{BaF}_2$  detectors. To evaluate the degree of suppression of the fringing field at the  $\text{BaF}_2$  detectors, energy spectra of  $^{241}\text{Am}$  ( $E_\gamma = 59.5$  keV) placed in the center of a conventional C-type magnet, in the center of the present cage-type magnet and without a magnetic field were taken by one of the  $\text{BaF}_2$  detectors placed 3 cm away from the source. As shown in Fig. 6, a drastic improvement from the conventional C-type magnet was achieved in the

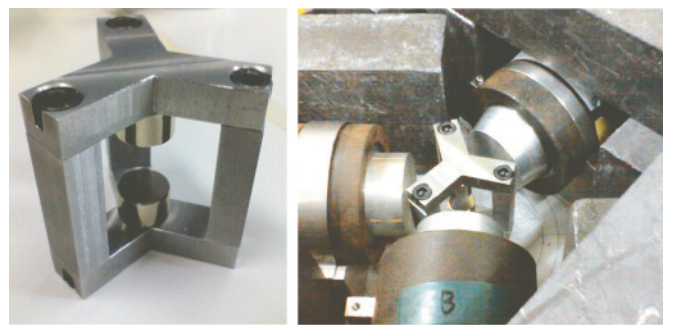


FIG. 5. (Color online) Appearance of the “cage type” magnet (left) and the set up of this magnet for the TDPAC measurement (right). Three return yokes were prepared every  $120^\circ$  for suppressing the fringing field. Three  $\text{BaF}_2$  detectors were placed 3 cm away from the center.

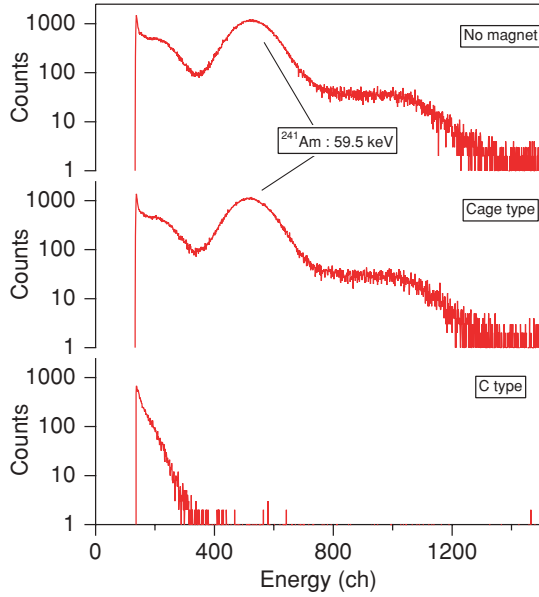


FIG. 6. (Color online) Energy spectra of the 59.5-keV  $\gamma$  ray of a  $^{241}\text{Am}$  source placed in different magnets taken by a  $\text{BaF}_2$  detector at 3 cm away from the source. “C type” denotes a conventional C-type magnet with the gap of 11 mm, “cage type” for the present cage-type magnet with a gap of 13 mm. Each magnet had the same magnetic field of 0.3 T at the gap center. “No magnet” is the spectrum without a magnetic field for comparison.

energy spectrum with the “cage type” magnet. The effect of the fringing field was eventually eliminated in the present measurement by using this magnet.

Three  $1.5\phi \times 1$ -inch-thick  $\text{BaF}_2$  counters were placed 3 cm away from the sample to form  $\pm 135^\circ$  in a plane perpendicular to the external magnetic field. Time spectra between signals from the detector at  $0^\circ$  and those at  $\pm 135^\circ$  were obtained. With the present detector arrangement, the time dependence of the asymmetry is given as follows:

$$\begin{aligned} R_{\pm}(t) &= \frac{N_{\pm}(t, \mp 135) - N_{\pm}(t, \pm 135)}{N_{\pm}(t, \mp 135) + N_{\pm}(t, \pm 135)} \\ &= \frac{3}{4} A_{22} \sin(\pm 2\omega_L t), \end{aligned} \quad (1)$$

where  $N_{\pm}(t, \alpha)$  is the number of coincidences between the two  $\gamma$  rays at 0 and  $\alpha$  degrees, and the subscript  $\pm$  in Eq. (1) stands for the direction of the external magnetic field. The constant coefficient,  $A_{22}$ , is the value determined by the multiplicities of  $\gamma$  rays and the spins of nuclear states involved in the cascade. The  $A_{22}$  value for the 228.2- to 49.7-keV  $\gamma$ - $\gamma$  angular correlation in  $^{132}\text{I}$  was calculated to be  $-0.07$  from the known spin values and the pure  $E2$ - $M1$  transitions in this cascade. Singh *et al.* reported an experimentally determined  $A_{22}$  value of  $-0.0608 \pm 0.0067$  [8], which is very consistent with the calculated value. The Larmor frequency,  $\omega_L$ , is given as

$$\omega_L = -\frac{\mu B}{I\hbar}, \quad (2)$$

where  $\mu$  and  $I$  are the magnetic moment and the spin of this state, respectively, and  $B$  is the magnetic field at the nucleus.

We performed two runs of the TDPAC measurements by inverting the direction of the external magnetic field along with the sample. The perturbation pattern must change its phase by  $180^\circ$  when only the magnetic field direction along with the sample is inverted and the other arrangements are untouched. This situation is easily realized by turning upside-down the magnet with the sample attached. Then, one obtains the enhanced asymmetry change by subtraction as

$$\begin{aligned} R_+(t) - R_-(t) &= 2R_+(t) \\ &= \frac{3}{2} A_{22} \sin(+2\omega_L t). \end{aligned} \quad (3)$$

A typical TDPAC spectrum is shown in Fig. 7. A constant offset is seen, which can be understood as being the result of a biased distribution of  $^{132}\text{I}$  in the nickel foil. Each selected piece in the sample preparation was confirmed to be only of dominant implantation of  $^{132}\text{Te}$ ; thus, it was not necessarily irradiated uniformly by the  $A = 132$  beam. Under such a biased distribution, the anisotropy is not canceled, because the biased distribution is also inverted in the inversion procedure described above. However, the beams of adjacent masses, which seriously affect the time spectrum around the prompt position, spread rather uniformly over the nickel foil because these are the overlap of halo-like components in the beams of adjacent masses in both sides of the primary beam of  $A = 132$ , thus the isotropic distribution is expected for  $\gamma$  rays from the nuclei of adjacent masses in the foils. This rather uniform distribution of the background components in the sample brings  $R_+(t) - R_-(t)$  close to zero at around  $t = 0$ . Therefore, the data within 0.45 ns from  $t = 0$ , corresponding to the HWHM of the time resolution, were excluded from the fit, and the Larmor frequency was derived from this pattern as  $\omega_L = -2\pi \times (140.4 \pm 11.7)$  Mrad/s. The sign of the Larmor

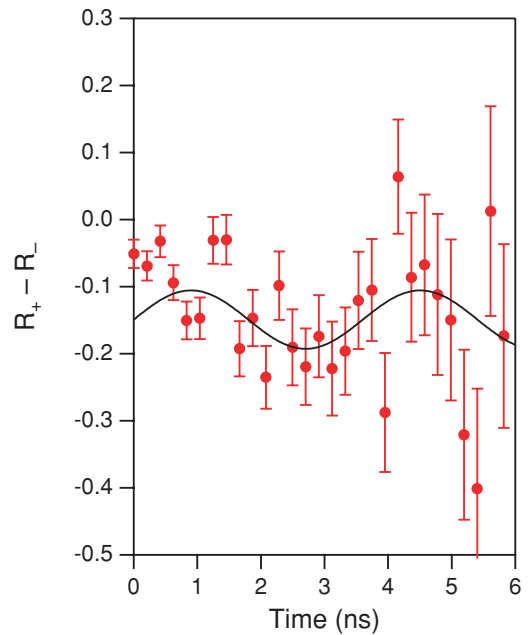


FIG. 7. (Color online) TDPAC spectrum of  $^{132}\text{I}$  in nickel. The data within HWHM determined in the half-life measurement from the prompt position was excluded for the fit.

TABLE I. Magnetic moment of the first excited state in  $^{132}\text{I}$ .

$\omega_L$	$-2\pi \times (140.4 \pm 11.7) \text{ Mrad/s}$
$B_{\text{hf}}$	$+26.5 \pm 0.5 \text{ T}$
$B_{\text{ext}}$	$0.3 \text{ T}$
$I^\pi$	$3^+$
$\mu(E_x = 49.7 \text{ keV}, I^\pi = 3^+)$	$+(2.06 \pm 0.18) \mu_N$

frequency is negative from the negative sign of  $A_{22}$  and the positive sign of the observed PAC pattern,  $R_+(t) - R_-(t)$ .

A theoretical approach to the hyperfine field by Akai *et al.* succeeded to reproduce the overall trend of hyperfine fields versus the impurity atom number, especially in the region of nontransition elements [14]. In their calculation, the sign of the hyperfine field at the iodine site in nickel is given to be positive. By taking this positive sign of the hyperfine field, the magnetic moment of the first excited state in  $^{132}\text{I}$  is determined to be  $\mu = +(2.06 \pm 0.18) \mu_N$ .

The sign of the hyperfine field at the iodine site in nickel can be experimentally deduced from our PAC spectrum by relying on the sign, not the magnitude, of the magnetic moment determined by Singh *et al.* The sign of the magnetic moment determined in their measurement is considered as to be reliable, because only an external magnetic field was used in their TIPAC measurement. By taking the positive sign of the magnetic moment by Singh *et al.*, the Larmor frequency observed in our measurement should take the opposite sign to the hyperfine field at the iodine site. Then, the sign of the hyperfine field at the iodine site in nickel is deduced to be positive, which is consistent with the sign given by Akai *et al.*

### III. DISCUSSIONS

A big question concerning in the first excited state in  $^{132}\text{I}$  is the inconsistent results on its half-life reported by several groups. Typical reported values of the half-life of this state are summarized in Table II. The present result shows a good agreement with that reported by Gorodetzky *et al.*

The reliability of the present result on the half-life should be carefully examined, because of the inconsistent results reported up to now. As shown in Fig. 4, we properly performed the selection of the objective  $\gamma$ -ray cascade, i.e., the decay spectrum was observed only when the  $\gamma$ -ray cascade of the first excited state in  $^{132}\text{I}$  was selected. We also paid attention to the time resolution of the measurement system. A sufficiently

 TABLE II. Typical reported values of the half-life of the first excited state in  $^{132}\text{I}$ .

	$T_{1/2}$ (ns)	Ref.
Gorodetzky <i>et al.</i>	$0.96 \pm 0.04$	[5]
Yousif <i>et al.</i>	$7.14 \pm 0.14$	[6]
Das <i>et al.</i>	$2.94 \pm 0.11$	[7]
Present	$1.120 \pm 0.015$	

 TABLE III. Magnetic moment of the first excited state in  $^{132}\text{I}$ . The calculated magnetic moment values with Eq. (4) in the text along with the averaged magnetic moment values for certain configurations are also shown in this table. All experimental values for empirical  $g$  factors are from [18].

	$\mu$ ( $\mu_N$ )	Ref.
Experiment	$+2.06 \pm 0.18$ $+2.22 \pm 0.30$	This work [8]
Calculation		
$(\pi g_{7/2})(\nu d_{3/2})^{-1}$	+2.40	
$(\pi d_{5/2})(\nu d_{3/2})^{-1}$	+2.83	
Values for empirical $g$ factors		
$(\pi g_{7/2})$	+2.80	Av. $^{131,133}\text{I}$
$(\pi d_{5/2})$	+2.81	Av. $^{129,131}\text{I}$
$(\nu d_{3/2})^{-1}$	+0.75	Av. $^{131}\text{Te}, ^{133}\text{Xe}$

high time resolution of the measurement system should be achieved in measurements of the half-life comparable to the time resolution of the detection system. Thanks to a good timing property of BaF<sub>2</sub> detectors, a sufficient time resolution for the present  $\gamma$ -ray cascade was obtained in our measurement system, as shown in Fig. 4. Based on these observations and considerations, we safely conclude that the half-life of the first excited state in  $^{132}\text{I}$  is  $1.120 \pm 0.015$  ns.

The transition probability,  $B(M1)$ , was deduced to be 0.024 W.u., from the present half-life value, the internal conversion coefficient  $\alpha = 5.62$ , calculated by BrIcc [15], and the fact that the transition is pure  $M1$  [16]. This small  $B(M1)$  value may indicate a large  $M1$  retardation for this state.

From the systematics observed in odd- $A$  isotopes of I, Te, and Xe, the configurations of the ground state and the first excited states in  $^{132}\text{I}$  are expected to be both mainly described as  $(\pi g_{7/2})(\nu d_{3/2})^{-1}$  with an admixture of  $(\pi d_{5/2})(\nu d_{3/2})^{-1}$ . From this point of view, the magnetic moments for the respective configurations are estimated and compared with the presently measured magnetic moment.

The magnetic moment of an odd-odd nucleus is described based on a simple  $jj$ -coupling model with empirical  $g$  factors [17] as

$$\mu(Z, N) = \frac{1}{2}(g_p + g_n)I + (g_p - g_n) \frac{j_p(j_p + 1) - j_n(j_n + 1)}{2(I + 1)}, \quad (4)$$

where  $I$ ,  $j_p$ , and  $j_n$  are the spins of the odd-odd, proton-odd, and neutron-odd nuclei,  $g_p$  and  $g_n$  are empirical  $g$  factors estimated from neighboring proton-odd and neutron-odd nuclei, respectively, by taking averages of the magnetic moment values for those nuclei. The values of magnetic moments for  $(\pi g_{7/2})(\nu d_{3/2})^{-1}$  and  $(\pi d_{5/2})(\nu d_{3/2})^{-1}$  are derived as +2.40 and +2.83, respectively. The present experimental result,  $\mu = +(2.06 \pm 0.18) \mu_N$ , is considered to be already well explained by  $(\pi g_{7/2})(\nu d_{3/2})^{-1}$ , taking into account the fact that the present  $jj$ -coupling model is very simple.

As for the configuration of this state, its quadrupole moment was measured by Ooms *et al.* [19], but they concluded that the main configuration was not specified due to the insufficient precision of their result.

Therefore, more precise measurements on the magnetic moment and the quadrupole moment along with theoretical calculations based on more realistic models should be performed for this state.

#### IV. CONCLUSION

The half-life and magnetic moment of the first excited state in  $^{132}\text{I}$  have been determined by using a radioactive beam from the RF-IGISOL at Tohoku University. The half-life and the magnetic moment of this level were determined to be  $T_{1/2} = 1.120 \pm 0.015$  ns and  $\mu = +(2.06 \pm 0.18)\mu_N$ , respectively. The present results are consistent with the half-life value obtained by Gorodetzky *et al.* and the magnetic moment value obtained by Singh *et al.* The present magnetic moment value is consistent with the value obtained from

a simple *jj*-coupling model in which the configuration of  $(\pi g_{7/2})(\nu d_{3/2})^{-1}$  is assumed for this state.

This is the first successful extraction of a radioactive beam in the region around  $^{132}\text{Sn}$  from the RF-IGISOL at Tohoku University. We will extend magnetic moment measurements in this region with radioactive beams produced by the RF-IGISOL.

#### ACKNOWLEDGMENTS

The authors are grateful to the technical staff members at SHI Accelerator Service Ltd. for the operation of the AVF cyclotron and beam handling. One of the authors (M.T.) is also grateful to Mr. Kanayama and Mr. Tsubokura at the machine shop in the Research Reactor Institute, Kyoto University for fabricating the cage-type magnet. This work was supported by Grant-in-Aid for Scientific Research(C) (19540291) from the Japan Society for the Promotion of Science (JSPS) and the Ministry of Education, Culture, Sports, Science and Technology (MEXT).

- 
- [1] B. A. Brown, N. J. Stone, J. R. Stone, I. S. Towner, and M. Hjorth-Jensen, *Phys. Rev. C* **71**, 044317 (2005).
  - [2] N. J. Stone, A. E. Stuchbery, M. Danchev, J. Pavan, C. L. Timlin, C. Baktash, C. Barton, J. R. Beene, N. Benczer-Koller, C. R. Bingham *et al.*, *Eur. Phys. J. A* **25**, 205 (2005).
  - [3] C. Goodin, N. J. Stone, A. V. Ramayya, A. V. Daniel, J. R. Stone, J. H. Hamilton, K. Li, J. K. Hwang, Y. X. Luo, J. O. Rasmussen *et al.*, *Phys. Rev. C* **78**, 044331 (2008).
  - [4] C. Goodin, J. R. Stone, N. J. Stone, A. V. Ramayya, A. V. Daniel, J. H. Hamilton, K. Li, J. K. Hwang, G. M. Ter-Akopian, and J. O. Rasmussen, *Phys. Rev. C* **79**, 034316 (2009).
  - [5] S. Gorodetzky, N. Schulz, J. Chevallier, and A. C. Knipper, *J. Phys. (Paris)* **27**, 521 (1966).
  - [6] A. A. Yousif, W. D. Hamilton, and E. Michelakakis, *J. Phys. G* **7**, 445 (1981).
  - [7] S. K. Das, R. Guin, and S. K. Saha, *Eur. Phys. J. A* **4**, 1 (1999).
  - [8] V. Singh, P. N. Tandon, S. H. Devare, and H. G. Devare, *Nucl. Phys. A* **132**, 221 (1969).
  - [9] W. Sato, H. Ueno, H. Watanabe, H. Miyoshi, A. Yoshimi, D. Kameda, T. Ito, K. Shimada, J. Kaihara, S. Suda *et al.*, *J. Phys. Soc. Jpn.* **77**, 095001 (2008).
  - [10] W. Sato, H. Ueno, H. Watanabe, H. Miyoshi, A. Yoshimi, D. Kameda, T. Ito, K. Shimada, J. Kaihara, S. Suda *et al.*, *Nucl. Instrum. Methods B* **266**, 316 (2008).
  - [11] Y. Miyashita, T. Wakui, N. Sato, A. Yamazaki, T. Endo, M. Fujita, A. Goto, S. Kinoshita, T. Koike, Y. Ma *et al.*, *Nucl. Instrum. Methods B* **266**, 4498 (2008).
  - [12] T. Sonoda, M. Fujita, A. Yamazaki, T. Endo, T. Shinozuka, Y. Miyashita, N. Sato, A. Goto, E. Tanaka, T. Suzuki *et al.*, *Nucl. Instrum. Methods B* **254**, 295 (2007).
  - [13] S. R. Reintsema, H. Waard, and S. A. Drentje, *Hyp. Int.* **2**, 367 (1976).
  - [14] H. Akai, M. Akai, S. Blügel, B. Drittler, H. Ebert, K. Terakura, R. Zeller, and P. Dederichs, *Prog. Theor. Phys. Suppl.* **101**, 11 (1990).
  - [15] T. Kibédi, T. Burrows, M. Trzhaskovskaya, P. Davidson, and C. W. Nestor Jr., *Nucl. Instrum. Methods A* **589**, 202 (2008), <http://www.rsphysse.anu.edu.au/nuclear/briccl/>.
  - [16] Y. Sergeenkov, *Nucl. Data Sheets* **65**, 277 (1992).
  - [17] H. M. Schwartz, *Phys. Rev.* **89**, 1293 (1953).
  - [18] N. Stone, *At. Data Nucl. Data Tables* **90**, 75 (2005).
  - [19] H. Ooms, J. Claes, F. Namavar, H. V. de Voorde, and M. Rots, *Nucl. Phys. A* **321**, 180 (1979).